

Capacitive electrodes based on a combination of activated carbon and graphene

Sh. Nurbolat^{1,2*} , M. Gabdullin³ , Zh. Kalkozova² ,
M. Mirzaeian⁴  and Kh. Abdullin² 

¹Almaty University of Power Engineering and Telecommunication, Almaty, Kazakhstan

²Al-Farabi Kazakh National University, Almaty, Kazakhstan

³Kazakh-British Technical University, Almaty, Kazakhstan

⁴School of Computing, Engineering and Physical Sciences, University of the West of Scotland, Paisley, UK

*e-mail: shyryn0709@gmail.com

(Received 27 September 2022; received in revised form 5 December; accepted 24 December 2022)

As an important element of energy storage systems, Supercapacitors are energy storage devices with high power density. The optimal materials and designs for supercapacitors are currently being studied very intensively, and despite many years of research in this area, the development of electrode materials with optimal properties problem remains very relevant. In order to ensure their high efficiency, along with a high specific capacitance, it is important to lower their series resistance. Carbon materials with a high specific surface area have been widely used as potential electrode material for supercapacitors, however their insufficiently low electrical resistivity limits the energy and power density of the device. Therefore, for optimizing the energy storage and power capability of supercapacitors, development of composite materials electrodes with optimized properties and low electric resistance is crucial. In this article, composite electrodes based on a combination of activated carbon and graphene are obtained and their properties are investigated. The capacitive performance of the composite electrodes is tested in an electrochemical cell and their advantage for lowering the electrical resistance of the device is shown.

Keywords: supercapacitors, energy storage, electrodes, graphene, carbon.

PACS number: 81.05.ue

1 Introduction

Renewable energy is rapidly developing at the present time. Various types of renewable green energy, such as solar photovoltaics, tidal and wind energies, show intermittent activity that depends on the time of day, season and weather. Therefore, energy storage and accumulation devices that dampen surges in the supply and consumption of electricity and ensure the security of the supply are necessary for the creation of modern energy systems and our future energy demands. An important role in such energy storage and accumulation systems is played by electrochemical devices, which are also widely used to power different electrical systems such as electric vehicles, electric autonomous devices, and various electrical gadgets [1-2].

Batteries and electrochemical capacitors are at the forefront of electrical energy storage technologies. Electrochemical batteries, in

particular lithium-ion batteries are technologies with high energy density and maximum specific energy storage capacity. While supercapacitors, which are the most important element of energy storage and accumulation systems, have the highest specific power. In electrochemical double layer capacitors (also called supercapacitors), energy is stored in the form of opposite electric charges on electrodes separated by a separator creating an electric double layer at the electrode/electrolyte interface [3-5]. They store more energy than ordinary capacitors and since charge carriers on a double charged layer do not cross the electrode-electrolyte interface during charge-discharge processes, supercapacitors have very high stability during cyclic operation with a very fast accumulation and release of charge during charge/discharge. The specific capacitance of the device is determined by the amount of charge that can be accumulated on the electrode surface, and

therefore the specific surface area of electrode is an important factor that determines the capacitance [6].

Supercapacitor technology has been intensively developed due to its high practical importance. However, despite of a significant research in the development of high energy supercapacitors in recent years, their performance to address the gap in the energy/power requirements of energy systems is not achieved yet [7-9].

Carbon-based nanostructured materials are very promising for the manufacture of electrochemical supercapacitors due to their significantly high specific surface area. Supercapacitors based on different carbon materials, such as activated carbon [10], graphene [11], reduced graphene oxide composites [12], carbon nanotubes [13–15], composites of graphene and carbon nanotubes [16], various carbon particles with developed morphology and high crystallinity, mesoporous carbon [17], doped porous carbon [18] with low electrical resistance are used as electrode materials for supercapacitors to improve the performance of their by lowering the electrical resistance of the electrodes. Li *et al.*, and Bukhari *et al.*, have also used carbon matrix to create a hybrid electrode material for supercapacitor electrodes [19, 20].

In order to improve the charge/discharge rate capability of the device by lowering the electric resistance of the electrodes and at the same time, maintaining its capacitance high by keeping the specific surface area of the carbon used as electroactive material, the fabrication of electrodes from carbon matrix composites is of high practical importance. This paper presents the results on the development of asymmetric supercapacitors using capacitive composite electrodes obtained from activated carbon and reduced graphene oxide.

2 Experiment details

The electrodes were made from activated carbon powder and graphene oxide. Commercial activated carbon had a surface area of $1800 \text{ m}^2\text{g}^{-1}$ according to the manufacturer's certificate. The surface area of the activated carbon used in this work was measured by the BET method (Brunauer-Emmett-Teller Method) and amounted to $1718 \text{ m}^2\text{g}^{-1}$. Graphene oxide (GO) was obtained by a modified Hummers method [21]. The reduction of graphene oxide was carried out by annealing in vacuum at temperatures from 110°C to 500°C and irradiation with UV radiation. To obtain reduced graphene oxide (rGO) by irradiation with UV light, a DRT 400 mercury lamp fed was used. The

lamp was fixed in a horizontal position 10 cm above the sample. The reduction of GO was monitored by XRD using a MiniFlex Rigaku diffractometer and by measuring the electrical resistance of GO layers. The GO layers were created by depositing a thin layer of an aqueous GO suspension on a $76 \times 26 \text{ mm}^2$ glass substrate, followed by drying at $\sim 100^\circ\text{C}$ under atmospheric conditions. Then the glass substrate was cut into samples of the required size for further studies. The electrical resistance of the GO layers was measured with a Keithley Instruments 6517B electrometer. The morphology of the samples was studied using a Quanta 200i 3D scanning electron microscope (SEM).

Electrode were fabricated using $\sim 80 \text{ wt}\%$ mixture of activated carbon and rGO as active material, $\sim 10 \text{ wt}\%$ carbon black as conductivity enhancer and $\sim 10\%$ polyvinylidene fluoride (PVDF) as binder. Acetone was used as a PVDF solvent. Nickel foam was used as conductive substrates for capacitive electrodes. A uniform paste was produced by mixing the electrode constituents in acetone for 3 h under magnetic stirring. The paste was then applied on nickel foam substrate. A two-electrode cell was then constructed using the fabricated electrodes with paper filter as a separator between them where an electrolyte comprising a KOH solution (3.5M) was added to the separator. The electrochemical performance of the cell was measured using an Elins P-40X-FRA-24M potentiostat.

3 Results and discussion

Figures 1a and 1b show SEM images of the original graphene oxide GO and the reduced graphene oxide rGO. SEM images of activated carbon (AC) used in this work and carbon black, which serves to fill the voids between AC particles, are also shown in Figures 1c and 1d, respectively.

For XRD analysis and electrical measurements, GO films were formed on glass substrates. A volume of an aqueous GO emulsion of about $100 \mu\text{L}$ per 1 cm^2 was applied with a micropipette onto a previously degreased glass substrate. After the emulsion dried, a film about 5 microns thick was formed. XRD patterns of the GO sample (Figure 2, curve 1) indicate a large interplanar spacing between graphene GO planes and a high degree of oxidation of graphite obtained by the Hummers method. Annealing in vacuum at temperatures of 110°C (curve 2) and 500°C (curve 3) leads to a decrease in the distance between the graphene planes, which is an indication of the reduction of GO under vacuum. It should be noted that the decrease in the distance between graphene

planes occurs very slowly at annealing temperatures from 100 to $\sim 140^\circ\text{C}$, and upon annealing between 140 and 150°C , the distance between graphene planes is abruptly restored to values corresponding to graphite. This abrupt reduction corresponds to the desorption of oxidizing radicals intercalated

into graphite and the release of gases [20]. In this case, GO films lose their mechanical strength. For applied purposes, it is important to obtain strong and conductive films; for this, it is necessary to use the control of the electrical properties of films in the process of reduction.

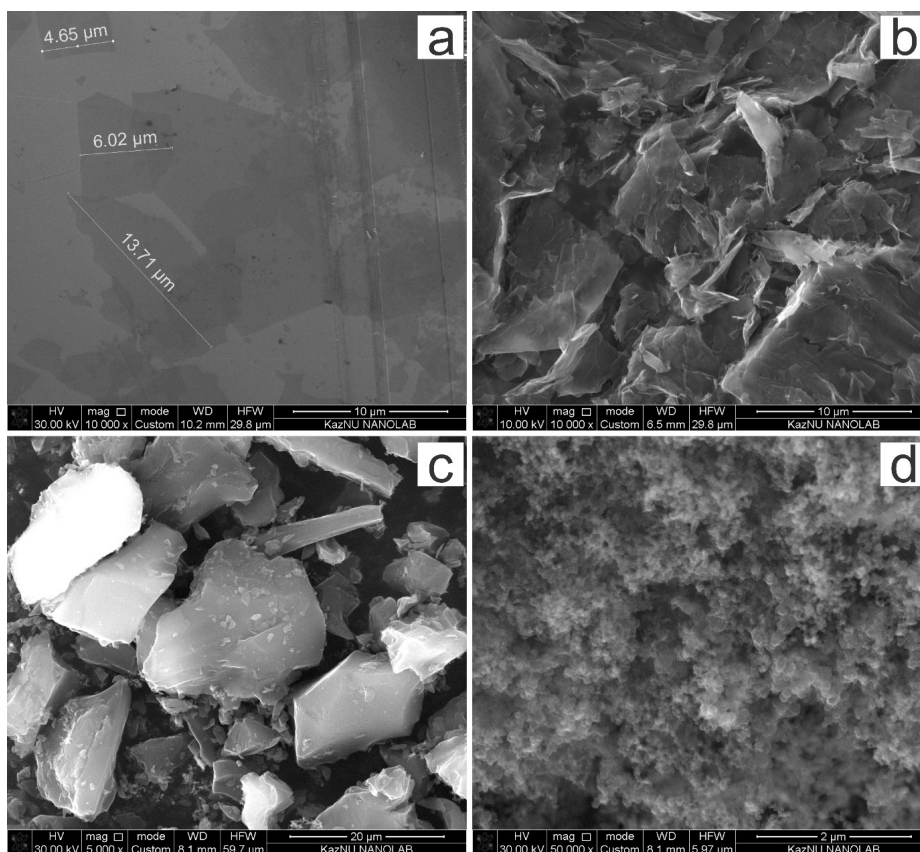


Figure 1 – SEM images of the carbon materials: (a) GO film on silicon substrate, (b) rGO, (c) activated carbon, and (d) carbon black

The original graphene oxide creates strong dielectric films on the substrate, by measuring the electrical resistance of the films, it is possible to monitor the GO reduction process at low ($100\text{--}110^\circ\text{C}$) temperatures with high sensitivity and determine the optimal reduction modes. To reduce GO, we used two methods: vacuum annealing and UV irradiation with a mercury lamp; the electrical resistance of the films was determined by the two-probe method.

It was found that vacuum annealing is much more efficient than annealing in air. For example, GO films remained dielectric after annealing in air at 110°C for 60 minutes, and after vacuum annealing at the same temperature, the electrical resistance dropped to $8 \times 10^8 \text{ Ohm}$. It is interesting to note that an increase in

the duration of vacuum annealing of the GO film did not lead to a further drop in its electrical resistance. It can be concluded that the drop in resistance of the film is presumably due to both thermal action, which causes desorption of a part of oxidizing radicals, and film compaction.

Another method used for reducing GO was UV light irradiation. Figure 3 shows the result of various combinations of exposure to vacuum annealing at $110^\circ\text{C}/60$ minutes and exposure to light from a mercury lamp. Curve 1 corresponds to the resistance of samples that were first annealed in vacuum at 110°C and then subjected to UV irradiation for up to 200 minutes. It can be seen that an increase in the time of UV irradiation leads to a progressive decrease in the electrical resistance of GO film.

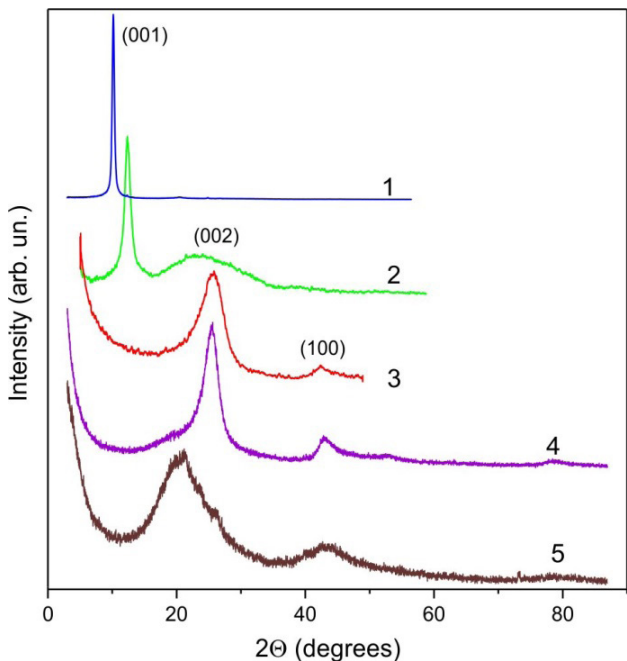


Figure 2 – XRD patterns of the carbon materials used: original GO (1), GO after vacuum annealing at 110°C (2) and 500°C (3), carbon black (4) and activated carbon (5)

It was found that when the sequence of operations is reversed, i.e., first irradiating the GO film with UV and then annealing it in vacuum at 110°C/60 minutes, the electrical resistance of the film decreases by approximately 3 orders of magnitude, as shown in Figure 3, curve 2. Moreover, if UV irradiation is carried out after vacuum annealing, then the electrical resistance of the films almost does not decrease (curve 3 in Figure 3). It can be concluded that vacuum treatment densifies the GO structure, which hinders the release of desorbing oxidative species from graphene oxide; therefore, such treatment should be applied at the final stage of obtaining rGO.

Despite the drop in the electrical resistance of rGO by many orders of magnitude compared to the original GO, the XRD data show insignificant but regular changes in the structure of rGO relative to GO, as can be seen from Figure 4. The intensity decreases, while the relative intensity of the (002) reflection increases.

The capacitive electrodes were made of AC activated carbon with rGO additives, acetylene black as a filler, polyvinylidene fluoride PVDF polymer as a reinforcing material, nickel foam serving as a substrate. In order to reduce the series resistance of the electrodes, rGO, which has a higher electrical conductivity, was added to the activated carbon. The resulting mixture was applied to a nickel foil substrate

with an area of 1×1 cm², which was thoroughly degreased beforehand. Two electrodes with the same mass were made in pairs.

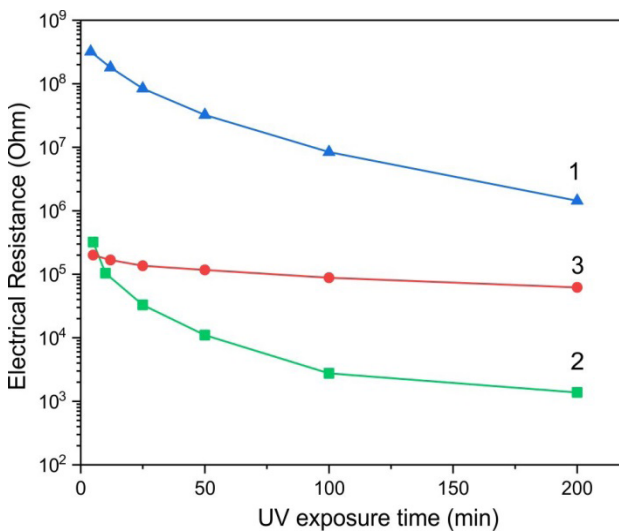


Figure 3 – Measurement of the electrical resistance of GO layers depending on the time of exposure to UV light: 1 – annealing in vacuum at 110°C followed by UV irradiation, 2 – UV irradiation followed by annealing at 110°C in vacuum, 3 – short-term (5 minutes) UV irradiation with subsequent annealing at 110°C in vacuum, followed by repeated UV irradiation

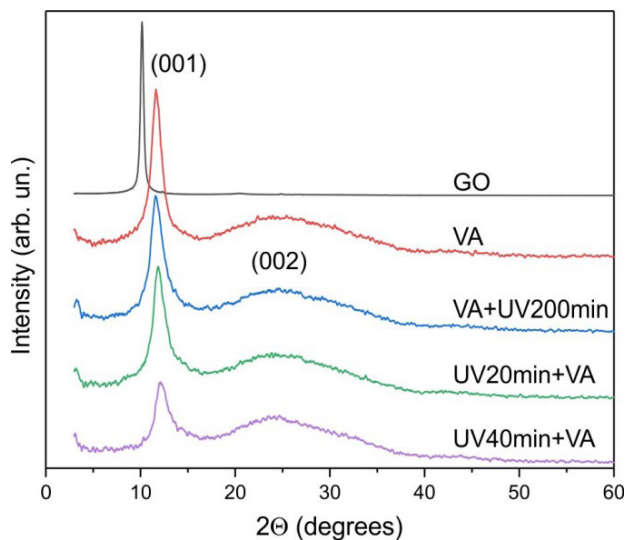


Figure 4 – XRD patterns of the graphene oxide: GO – as-synthesized GO, VA – vacuum annealing, VA+UV200min – vacuum annealing followed by irradiation with UV light for 200 min, UV20min+VA – irradiation with UV light for 20 min followed by vacuum annealing, UV40min+VA – irradiation with UV light for 40 min followed by vacuum annealing

Figure 5(a) shows the cyclic voltammograms of activated carbon (AC) and a mixture of AC : rGO = 10 : 1 (AC+Graphene) used as electroactive material with 3.5 M KOH electrolyte in the electrochemical capacitor measured at a sweep rate of 10 mV s⁻¹. It can be seen that the shape of the CV curves is close to rectangular, redox current peaks disappear, which corresponds to the purity density of the materials used. At the same time, for the AC + rGO capacitor, the CV curves are more rectangular than those for

the AC capacitor. This is due to their lower series resistance of the AC-rGO mixture as shown before.

Galvanostatic charge-discharge (GCD) curves normalized to a current of 1 A g⁻¹ (Figure 5 b) show that the capacitances of the AC and AC+rGO mixture capacitors are close, but the AC+rGO electrodes show less series resistance because the potential jump at the change in current direction is less than that of AC electrodes and correspond to a resistance of 6 ohms versus 10 ohms for AC electrodes.

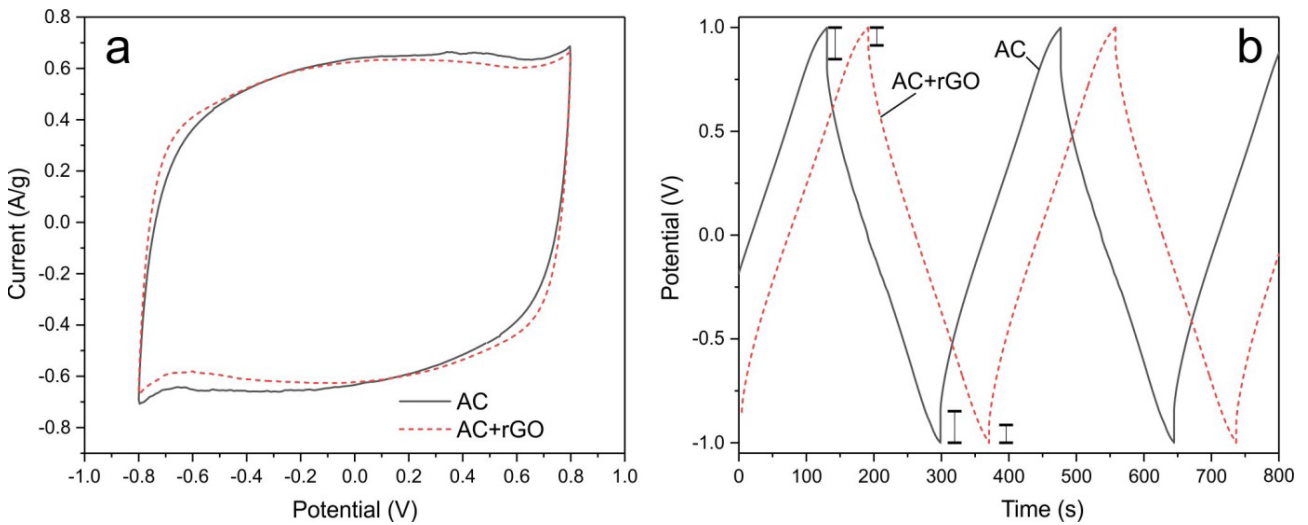


Figure 5 – Cyclic voltammograms of capacitors using activated carbon (AC) and a mixture of AC : rGO = 10 : 1 (AC+rGO) as electrode material (a); GCD curves of activated carbon (AC) and mixture (AC+rGO) capacitors at 1 A g⁻¹ current (b)

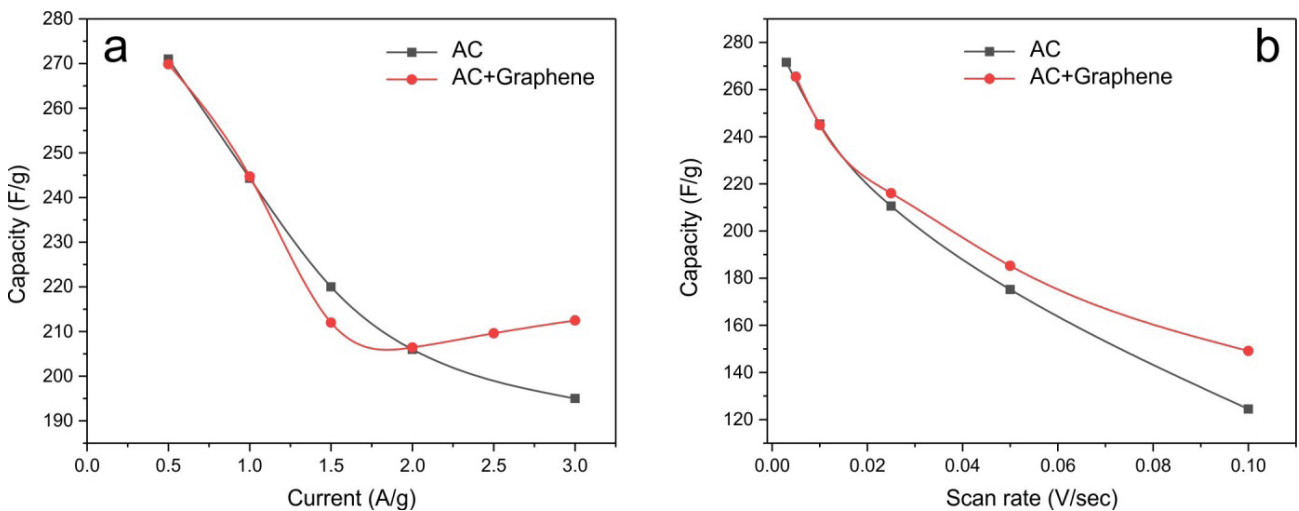


Figure 6 – The dependence of the capacitance of capacitors obtained from the current-voltage curves (a) and the galvanostatic charge-discharge curves (b)

Figure 6 shows graphs of capacitor capacitance changes with increasing galvanostatic charge-discharge GCD (Figure 6a) and increasing scan rate when measuring CV cyclic voltammograms (Figure 6b). It can be seen that the addition of graphene slows down the capacitance drop at high sweep rates for the CV curves and at high currents for the GCD curves. Thus, the presence of graphene improves performance in the high current region, that is, in the working region of supercapacitors, by improving the electrical characteristics of the material.

The specific capacitance of carbon capacitors also decreases with an increase in the mass of the electrode load, and this is a significant technical problem. The CV curves measured at low sweep rates for electrode loads in the range of 10 to 100 mg cm⁻² are almost the same, however, as the potential scan rate increases, the electrodes with higher load masses show faster capacitance drops much faster for high load masses.

4 Conclusions

The drop in specific capacitance is due to an increase in the thickness of the carbon layer and, accordingly, an increase in the electrical resistance of the electrode. Series electrical resistance also limits

the power of the capacitor. In thinner electrodes, the charge distribution in the electrode layer is kept the same and the contribution of the entire electrode to the capacitance is uniform, however with increase in the electrode's thickness, the charge distribution in the electrode depth varies and the contribution to the capacitance of regions remote from the surface in contact with the metal current collector decreases, and therefore in order to maintain their capacitive contribution, long charge-discharge times are required. This could be considered as one of the main advantages of supercapacitors which allows maintaining release of energy in different time scales to respond to the energy demands in a range of delivery times where, high developed powers, are leveled. The creation of a mixture of activated carbon and graphene with different ratios could contribute to a decrease in electrical resistance improving the energy/power response characteristics of capacitors in the energy continuum demands.

Acknowledgements

This research was funded by Ministry of Education and Science of the Republic of Kazakhstan, grant number AP09259253.

References

1. Zh. Jingyuan, B. Andrew. Review on supercapacitors: Technologies and performance evaluation // *Journal of Energy Chemistry*. – 2021. – Vol. 59. – P.276–291. <http://doi:10.1016/j.jechem.2020.11.013>.
2. A. González, E. Goikolea, J. A. Barrena and R. Mysyk. Review on supercapacitors Technologies and material // *Renewable and Sustainable Energy Reviews* – 2016. – Vol. 17. – P. 1189–1206. <http://dx.doi.org/10.1016/j.rser.2015.12.249>.
3. P. Naskar, D. Kundu, A. Maiti, P. Chakraborty, B. Biswas, and A. Banerjee. Frontiers in Hybrid Ion Capacitors: A Review on Advanced Materials and Emerging Devices // *ChemElectroChem*. – 2021. – Vol. 36. – P.1393–1429. <http://doi.org/10.1002/celec.202100029>.
4. M. E. Sahin, F. Blaabjerg, A. Sangwongwanich. A Comprehensive Review on Supercapacitor Applications and Developments // *Energies* – 2022. . – Vol. 15. – P. 674. <https://doi.org/10.3390/en15030674>.
5. S. Huang, X. Zhu, S. Sarkar, and Y. Zhao. Challenges and opportunities for supercapacitors // *APL Mater.* – 2019. – Vol. 7. – P. 100901. <http://doi.org/10.1063/1.5116146>.
6. G.A. Tafete, M.K. Abera, G. Thothadri. Review on nanocellulose-based materials for supercapacitors applications // *J. Energy Storage*. – 2022. – Vol. 48. – P. 103938. <https://doi.org/10.1016/j.est.2021.103938>
7. Y. Zhang, L. Cheng, L. Zhang, D. Yang, C. Du, L. Wan, J. Chen, M. Xie. Effect of conjugation level on the performance of porphyrin polymer based supercapacitors // *J. Energy Storage*. – 2022. – Vol. 34. – P. 102018. <https://doi.org/10.1016/j.est.2020.102018>
8. S. Faraji, F. N. Ani. The development supercapacitor from activated carbon by electroless plating—A review // *Renewable and Sustainable Energy Review*. – 2015. – Vol. 42. – P.823-834. <https://doi.org/10.1016/j.rser.2014.10.068>
9. S.Dhibar, S.Malik. Morphological Modulation of Conducting Polymer Nanocomposites with Nickel Cobaltite/Reduced Graphene Oxide and Their Subtle Effects on the Capacitive Behaviors // *ACS Applied Materials & Interfaces*. – 2020. – Vol. 15. – P. 54053-54067. <https://doi.org/10.1021/acsami.0c14478>
10. I.P. Prado, D.S. Torres, R.R.Rosas, E. Morallón and D. C.Amorós. Design of Activated Carbon/Activated Carbon Asymmetric Capacitors // *Frontiers in Materials*. – 2016. – Vol. 12. <https://doi.org/10.3389/fmats.2016.00016>

11. W. K. Chee, H. N. Lim, Z. Zainal, N. M. Huang, I. Harrison, Y. Andou. Flexible Graphene-Based Supercapacitors A Review // *J. Phys. Chem.* – 2016. – Vol. 19. – P. 4153–4172. <https://doi.org/10.1021/acs.jpcc.5b10187>.
12. M. Rapisarda, F. Marken, M. Meo. Graphene oxide and starch gel as a hybrid binder for environmentally friendly high-performance supercapacitors // *Communications Chemistry.* – 2021. – Vol. 11. – P. 169. <https://doi.org/10.1038/s42004-021-00604-0>
13. Z.Lu, R.Raad, F.Safaei, J.Xi, Z.Liu, J.Foroughi. Carbon Nanotube Based Fiber Supercapacitor as Wearable Energy Storage // *Frontiers in Materials.* – 2019. – Vol. 14. <https://doi.org/10.3389/fmats.2019.00138>.
14. W. Liang, I. Zhitomirsky. Composite Ti₃C₂T_x-carbon nanotube electrodes with high active mass for supercapacitors // *Open Ceramics.* – 2021. – Vol. 4. – P. 100158. <https://doi.org/10.1016/j.oceram.2021.100158>.
15. S.Wang, Y.Liang, W.Zhuo, H.Lei, M.S. Javed, B.Liu, W.Mai. Freestanding polypyrrole/carbon nanotube electrodes with high mass loading for robust flexible supercapacitors // *Materials Chemistry Frontiers.* – 2021. – Vol. 5. – P. 1324–1329. <https://doi.org/10.1039/d0qm00649a>.
16. A. Aphale, K.Maisuria, M. Mahapatra, et al. Hybrid Electrodes by In-Situ Integration of Graphene and Carbon-Nanotubes in Polypyrrole for Supercapacitors // *Sci Rep.* – 2015. – Vol. 5. – P. 14445. <https://doi.org/10.1038/srep14445>.
17. S. Yuan, Q. Gao, C. Ke, T. Zuo, J. Hou, J. Zhang. Mesoporous Carbon Materials for Electrochemical Energy Storage and Conversion // *ChemElectroChem.* – 2021. – Vol. 9. <https://doi.org/10.1002/celec.202101182>.
18. K. Wei, F. Zhang, Y. Yang, B. Zhai, X. Wang, Y. Song. Oxygenated N-doped porous carbon derived from ammonium alginate: Facile synthesis and superior electrochemical performance for supercapacitor // *Journal of Energy Storage.* – 2022. – Vol. 51. – P. 104342. <https://doi.org/10.1016/j.est.2022.104342>.
19. Q.B. Le, T. Nguyen, H. Fei, C. Bubulinca. Electrochemical performance of composite electrodes based on rGO, Mn/Cu metal–organic frameworks, and PANI // *Scientific Reports.* – 2022. – Vol. 12. – P. 664. <https://doi.org/10.1038/s41598-021-04409-y>.
20. S. W. Bokhari, Y. Hao, A. H. Siddique, Y. Ma, M. Imtiaz, R. Butt, P. Hui, Yao Li, S. Zhu. Assembly of hybrid electrode rGO–CNC–MnO₂ for a high performance supercapacitor // *Results in Materials.* – 2019. – Vol. 5. – P.100007. <https://doi.org/10.1016/j.rinma.2019.100007>.
21. J. Chen, B. Yao, C. Li, G. Shi. An improved Hummers method for eco-friendly synthesis of graphene oxide // *Carbon* – 2013. – Vol. 4. – P. 225 – 229. <https://doi.org/10.1016/j.carbon.2013.07.055>

© This is an open access article under the (CC)BY-NC license (<https://creativecommons.org/licenses/bync/4.0/>).
Funded by Al-Farabi KazNU